Available online at www.sciencedirect.com
SCIENCE DIRECT®
International Journal of Heat and Fluid Flow 25 (2004) 128–139
International Journal of HEAT AND FLUID FLOW
www.elsevier.com/locate/ijhff

Boiling in microchannels: a review of experiment and theory

John R. Thome *

Laboratory of Heat and Mass Transfer (LTCM), Faculty of Engineering Science, Swiss Federal Institute of Technology Lausanne (EPFL), CH-1015 Lausanne, Switzerland

Abstract

A summary of recent research on boiling in microchannels is presented. The review addresses the topics of macroscale versus microscale heat transfer, two-phase flow regimes, flow boiling heat transfer results for microchannels, heat transfer mechanisms in microchannels and flow boiling models for microchannels. In microchannels, the most dominant flow regime appears to be the elongated bubble mode that can persist up to vapor qualities as high as 60–70% in microchannels, followed by annular flow. Flow boiling heat transfer coefficients have been shown experimentally to be dependent on heat flux and saturation pressure while only slightly dependent on mass velocity and vapor quality. Hence, these studies have concluded that nucleate boiling controls evaporation in microchannels. Instead, a recent analytical study has shown that transient evaporation of the thin liquid films surrounding elongated bubbles is the dominant heat transfer mechanism as opposed to nucleate boiling and is able to predict these trends in the experimental data. Newer experimental studies have further shown that there is in fact a significant effect of mass velocity and vapor quality on heat transfer when covering a broader range of conditions, including a sharp peak at low vapor qualities at high heat fluxes. Furthermore, it is concluded that macroscale models are not realistic for predicting flowing boiling coefficients in microchannels as the controlling mechanism is not nucleate boiling nor turbulent convection but is transient thin film evaporation (also, microchannel flows are typically laminar and not turbulent as assumed by macroscopic models). A more advanced *three-zone* flow boiling model for evaporation of elongated bubbles in microchannels is currently under development that so far qualitatively describes all these trends. Numerous fundamental aspects of two-phase flow and evaporation remain to be better understood and some of these aspects are also discussed.

Keywords: Boiling; Evaporation; Microchannels; Two-phase flow

1. Introduction

There are a growing number of experimental studies on two-phase flow and evaporation heat transfer in microchannels. Furthermore, the challenges of modelling the heat transfer process, prediction of flow pattern transitions (i.e. flow pattern map preparation) and calculation of two-phase pressure drops in microchannels have also been approached. These topics (with the exception of two-phase pressure drops) will be addressed here, in part to report what has been accomplished and secondly to address and identify some open issues. However, the state-of-the-art of two-phase flow and evaporation in microchannels is still in its initial development phase and what is presented here must be considered as a preliminary assessment, not as definitive information.

From a point of view of applications, microheat exchangers, microcooling assemblies and thermal systems implementing such devices, referred to as micro-thermal-mechanical systems (MTMS) as opposed to micro-electronic-mechanical-systems (MEMS), are rapidly advancing to ever smaller sizes. These are used as microcooling elements for electronic components, portable computer chips, radar and aerospace avionics components, and microchemical reactors. Besides single-phase cooling applications, numerous two-phase (evaporation) cooling applications are being identified, for now being implemented without the benefit of thermal design methods for heat transfer and pressure drops (a deficit which is overcome by extensive testing). In fact, what can now be fabricated, either by micromachining of silicon wafers or microextrusion of aluminum elements, has vastly outpaced what can be

* Tel.: +41-21-693-5981; fax: +41-21-693-5960.
E-mail address: john.thome@epfl.ch (J.R. Thome).

0142-727X/$ - see front matter © 2003 Elsevier Inc. All rights reserved.
doi:10.1016/j.ijheatfluidflow.2003.11.005

Nomenclature

a	constant, W/(m^2 K^n)
Co	confinement number
d_{bub}	bubble departure diameter, m
$d_{bub,F}$	Fritz bubble departure diameter, m
D	diameter, m
D_h	hydraulic diameter, m
F	Chen two-phase convection multiplier
g	acceleration of gravity, m/s^2
G	mass velocity, kg/m^2 s
h_{exp}	experimental heat transfer coefficient, W/m^2 K
h_L	liquid-phase heat transfer coefficient, W/m^2 K
h_{nb}	nucleate boiling heat transfer coefficient, W/m^2 K
h_{tp}	flow boiling heat transfer coefficient, W/m^2 K
h_{vapor}	vapor-phase heat transfer coefficient, W/m^2 K
h_{wet}	wet wall heat transfer coefficient, W/m^2 K
L_L	length of liquid slug, m
L_p	length of liquid slug/bubble pair, m
L_V	length of elongated bubble, m
m	mass velocity, kg/m^2 s
n	exponent
P_{sat}	saturation pressure, Pa
$(dP/dT)_{sat}$	slope of vapor pressure curve, Pa/K
q	heat flux, W/m^2
r_i	internal radius of tube, m
r_{nuc}	bubble nucleation radius, m
S	velocity ratio
S	Chen boiling suppression factor
ΔT	wall temperature, K
ΔT_{nuc}	nucleation temperature, K
x	vapor quality
δ	liquid film thickness, m
δ_{min}	minimum liquid thickness, m
δ_o	liquid film thickness, m
ε	cross-sectional void fraction of vapor
θ_{dry}	dry angle around top of tube in stratified type of flow, rad
ρ_G	vapor density, kg/m^3
ρ_L	liquid density, kg/m^3
σ	surface tension, N/m

thermally modelled. Also, while circular channels are the norm for macroscale evaporation processes, at the microscale non-circular channels are more common. Thus, significant advances are required for the optimal development and operation of these devices.

It is not the objective of this review to describe or mention all the work that has been published on this topic but instead to present some of the typical results and make an assessment of where we stand today. Thus, the reader is recommended to refer to other general reviews on microchannel heat transfer for single-phase and two-phase flows by Mehendal et al. (2000), Kandlikar (2001), Huo et al. (2001), Kandlikar and Grande (2003), Bergles et al. (2003) and Thome et al. (2003).

2. Macro-to-microscale transition in evaporation

From a practical point of view, it is necessary to be able to identify the lower limit of reliable applicability of macroscale design methods for evaporation processes, with respect to prediction of void fractions, heat transfer coefficients, flow pattern maps and two-phase pressure drops. Thus, it is important to address this threshold issue with respect to the process of evaporation, since the threshold for two-phase processes is not likely to be the same as that for single-phase processes. From a phenomenological viewpoint, some macroscale thermal and fluid phenomena may be suppressed or relegated to secondary importance by the decrease in channel size while others may be enhanced or newly created. Unfortunately, a recognized transition threshold criterion from macroscale to microscale is itself not yet very well defined for two-phase processes. In fact, this threshold question has not even been seriously investigated experimentally. Furthermore, some researchers propose to also include a mesoscale range between these two.

As phase-change heat transfer phenomena in microscale and macroscale show distinct differences, only part of the available knowledge about macroscale heat transfer can be transferred to the microscale, but it is not clear exactly what is still valid and what is not. Several classifications for the transition from macroscale to microscale heat transfer, based on the hydraulic diameter D_h for non-circular channels have been proposed. First, Mehendal et al. (2000) recommended a size classification as follows: microchannels (1–100 μm), mesochannels (100 μm to 1 mm), macrochannels (1–6 mm) and conventional channels ($D_h > 6$ mm) while Kandlikar (2001) recommends the following classification and size ranges: microchannels (50–600 μm), minichannels (600 μm to 3 mm) and conventional channels ($D_h > 3$ mm). Such transition criteria are arbitrary and do not reflect the influence of channel size on the physical mechanisms. For example, the effect of reduced pressure on bubble sizes and flow transitions. A more general definition should address the limit where classical theory

is no longer fully applicable with respect to the two-phase flow and heat transfer processes.

Such a macro-to-micro transition criterion might be related to the bubble departure diameter. That is, the point at which the bubble departure diameter reaches that of the flow channel, such that further growth is confined by the channel and only one bubble can exist in the channel cross-section at a time (as opposed to multiple bubbles in a macrochannel). Hence, the threshold to confined bubble flow could be taken as the microscale threshold. As a first approximation, one could take the bubble departure diameter in nucleate pool boiling without cross-flow. The Fritz (1935) equation gives this diameter $d_{\mathrm{bub,F}}$ as:

$$d_{\mathrm{bub,F}} = 0.0208\beta\left[\frac{\sigma}{g(\rho_{\mathrm{L}}-\rho_{\mathrm{G}})}\right]^{1/2} \tag{1}$$

where the contact angle β is in degrees (°), e.g. for R-134a at $T_{\mathrm{sat}} = 0$ °C and a contact angle assumed to be 22.5°, the bubble departure diameter is 0.67 mm. For application to high pressures, this expression has been expanded to:

$$d_{\mathrm{bub}} = 0.0012\left(\frac{\rho_{\mathrm{L}}-\rho_{\mathrm{G}}}{\rho_{\mathrm{G}}}\right)^{0.9} d_{\mathrm{bub,F}} \tag{2}$$

At very high pressures, bubble diameters are very small (of the order of 0.05 mm or less) and thus a 1.0 mm channel in that case looks large and a macroscale process probably still exists. The opposite is true at subatmospheric pressures where bubbles tend to be larger. For flow inside a tube, bubble departure is not controlled only by surface tension and buoyancy forces but also by shear effects. No general method is apparently available to describe this process in microchannels while various attempts have been made to model it in macrochannels, with limited success.

As a consequence, Kew and Cornwell (1997) recommend using a confinement number Co as a criterion to differentiate between macroscale and microscale two-phase flow and heat transfer, defined as

$$Co = \left[\frac{\sigma}{g(\rho_{\mathrm{L}}-\rho_{\mathrm{V}})D_{\mathrm{h}}^2}\right]^{1/2} \tag{3}$$

where D_{h} is the hydraulic diameter of the flow channel. They reported that the heat transfer and flow characteristics were significantly different than those observed in macrochannels for $Co > 0.5$. Hence, the criterion of $Co > 0.5$ is one possible proposal to consider. For example, for R-134a at $T_{\mathrm{sat}} = 0$ °C, the threshold diameter given by this criterion is 1.92 mm and becomes smaller as the saturation pressure increases.

Lin and Pisano (1991) have advanced another suggestion, that is to define the microchannel threshold as the point at which boiling nucleation is altogether suppressed, such that bubbles cannot form, where the nucleation radius r_{nuc} is predicted from the nucleation superheat equation

$$r_{\mathrm{nuc}} = \frac{2\sigma}{\Delta T_{\mathrm{nuc}}(\mathrm{d}P/\mathrm{d}T)_{\mathrm{sat}}} \tag{4}$$

and the nucleation superheat is ΔT_{nuc}. Since nucleation sites for bubble formation in heated channels are on the order of 1–2 μm or less, the criterion of $D_{\mathrm{h}} < 2r_{\mathrm{nuc}}$ is probably better assigned to the *microscale-to-nanoscale* threshold.

In summary, it seems most opportune to choose the threshold to confined bubble flow as the *interim* criterion for the threshold from macroscale to microscale until this question has been more completely satisfied. This is a likely condition below which macroscale heat transfer design methods would be expected to become unreliable for predicting flow boiling heat transfer coefficients and two-phase flow pattern transitions and hence this may thus be a workable threshold for when to stop applying macroscale methods and to begin applying microscale design methods. Another attenuating factor is the transition from turbulent flow to annular flow; essentially all macroscale prediction methods were developed from databases with turbulent flow occurring in the liquid phase while most microscale evaporation applications are at liquid Reynolds numbers below 2300. This turbulent versus laminar flow question superimposes itself on top of the macro-to-microscale evaporation problem.

3. Void fraction

The most influential parameter in two-phase flow and heat transfer is the void fraction of the vapor phase in the cross-section of the flow channel. Numerous analytical theories have been presented for predicting void fractions for two-phase flows in macrochannels and in particular for the bubble, slug, annular and stratified flow regimes. These are not presented here as they can be found in numerous reference books, such as Collier and Thome (1994). They are potentially applicable to microchannels for those same flow regimes. As the vapor and liquid phases do not travel at the same velocity (when they do, this is referred to as *homogeneous* flow), the void fraction and dynamics of the two-phase interface are a function of the flow itself. For instance, in an elongated bubble flow with individual bubbles separated by liquid slugs, if the slugs and bubbles travel at the same mean velocity then this would be a homogeneous flow, ignoring the slower velocity of the liquid film between the bubble and the channel wall. Assuming this, we can apply the homogeneous void fraction model to this regime in microchannels, which gives the cross-sectional vapor void fraction ε as:

$$\varepsilon = \frac{1}{1 + \left(\frac{1-x}{x}\right)\frac{\rho_G}{\rho_L} S} \tag{5a}$$

For a homogeneous flow, the velocity ratio (or slip ratio) $S = 1.0$. Since in general $S \geqslant 1.0$, this expression gives the upper limit to the actual void fraction and probably a reasonable estimate for this situation.

Obtaining accurate cross-sectional void fraction measurements in a microchannel is an experimental challenge. Several such studies are reported in the literature using various approaches but none are sufficiently accurate to propose any prediction methods. Also, it is important to mention here that it is the *cross-sectional* void fraction, not the *volumetric* void fraction, that is desired. Cross-sectional void fractions *cannot* be determined using the quick-closing valve method since that gives volumetric void fractions, which are equal to cross-sectional void fractions only when the two phases travel at the same velocity, i.e. the homogeneous case for which we already have Eq. (5a). The relationship between the cross-sectional void fraction ε and the volumetric void fraction ε_{Vol} can be obtained from their definitions:

$$\varepsilon_{Vol} = \frac{\varepsilon}{\frac{1}{S}(1-\varepsilon) + \varepsilon} \tag{5b}$$

Since $S \geqslant 1$, incorrectly using the volumetric void fraction ε_{Vol} in place of the cross-sectional void fraction ε overpredicts the latter's value, and in some cases gives void fractions larger than the homogeneous void fraction (for which $S = 1$).

4. Two-phase flow studies

In two-phase microchannel flows one important difference with respect to macrochannel flows is that the liquid flow is laminar at most but not all the test conditions, which is quite rare in macrochannel studies. The typical range of interest in microchannel flows are liquid Reynolds numbers from 100 to 4000. Hence, flow pattern transition theories with turbulent liquid flows cannot be expected to apply directly to the similar transition for laminar conditions. Capillary (surface tension) forces become important in small diameter tubes, eliminating stratification of the liquid and hence channel orientation is at most only of secondary importance in microchannels.

Before proceeding, several cautionary notes on two-phase flow observations should be made. First of all, not only are flow pattern observations subjective but also various research groups use different categories or names to describe the same thing, or use additional subcategories that others do not. Hence, similar to the macroscale situation, it is often not feasible to do a valid comparison between independent databases. Secondly, in gas–liquid flows the two phases must be mixed before entering the observation zone. To achieve this, sometimes a gas–liquid mixer is installed upstream of the observation zone or they are mixed in an entrance header prior to the microchannel. This raises a fundamental issue: Are the flow patterns observed representative of the flow or are they influenced by the geometry of the mixer or header? This is not any easy issue to resolve. Below, a selection of studies on flow pattern observations reported for microchannel flows are presented.

As an example of what microscale two-phase flows look like, Fig. 1 were taken from Feng and Serizawa

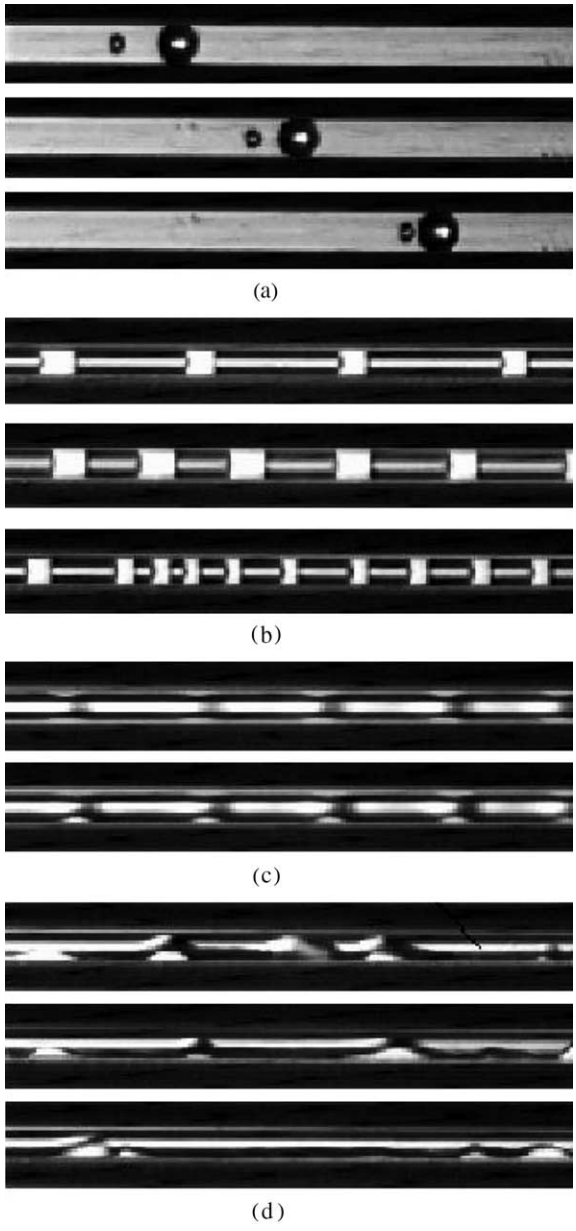

Fig. 1. Microchannel flow patterns observed by Feng and Serizawa (2000): (a) bubbly flow, (b) slug or elongated bubble flow, (c) liquid ring flow and (d) liquid lump flow.

(2000) that depict flow regimes observed in videos of air–water flowing in a 50 μm diameter, transparent channel whose refractive index is the same as water. They categorized their observations as follows: bubble flow, elongated bubble (or slug) flow, annular flow, liquid ring flow, liquid lump flow and mist flow. Liquid ring flow occurred as an additional flow pattern between elongated bubble flow and annular flow and hence is quite likely to be some type of intermediate transition regime. According to the comments of Feng and Serizawa, liquid ring flow apparently occurs when the pressure gradient across a liquid slug between two elongated bubbles is large enough to pierce it while the capillary, viscous and drag forces apparently resist the dissolution of the resulting thick liquid ring. They injected air into the water via a mixer upstream of the viewing zone with a relatively long developing length between their mixer and viewing zone. Yet, since it is difficult for elongated bubbles to coalesce in microchannels, it is not clear if the mixer imposes an effect on the resulting flow patterns and their transitions. The liquid ring and liquid lump regimes might be similar to those depicted by Triplett et al. (1999) who have instead identified them as slug–annular flow transitions for their gas–liquid tests.

Tran et al. (1996) observed two-phase flow patterns for R-12 in a 2.46 mm circular channel, noting that the transition from slug flow (elongated bubble flow) to annular flow occurred at much higher vapor qualities than typical of macrochannels, i.e. at $x \approx 0.6$–0.7 as opposed to $x \approx 0.25$–0.35 typical for macrochannel flows.

Regarding stratification effects, Triplett et al. (1999) reported that it never occurred in their investigations for geometries with internal dimensions from 1.09 to 1.49 mm for gas–liquid flows. On the other hand, Kasza et al. (1997) reported stratified flow at very low flow rates, in their case at 21 kg/m^2 s, but they used a relatively large rectangular flow channel of 2.5×6.0 mm with water, for which they also reported observations of bubbly flow and slug flow. Kuwahara et al. (2000) investigated R-134a evaporating in a 1.2 mm horizontal tube at mass velocities from 80 to 1260 kg/m^2 s and vapor qualities from 0.008 and 0.975, all at a saturation pressure of 0.92 bar. They observed the following flow regimes, which are also typical of macroscale tubes: bubbly flow, plug flow, slug flow, wavy-annular flow and annular flow. The wavy-annular flow means some stratification occurs, which is surprising. Their obserations compared poorly with macroscale flow pattern maps of Baker (1954) and Taitel and Dukler (1976) but they modified the Baker map to fit their observations.

Cornwell and Kew (1993, 1995) and Kew and Cornwell (1997) identified three different flow regimes in their work and that of others: isolated bubbles, confined bubbles and an annular slug flow regime plus partial dryout at some conditions. They introduced the confinement number Co described earlier. Presumably, their *confined bubble* label is equivalent to the *elongated bubble* or *slug flow* label used by others. Sheng and Palm (2000) performed flow boiling experiments with water in vertical glass tubes (1.0–4.0 mm diameter) and reported observing three flow regimes: isolated bubble flow, confined bubble flow and annular flow.

Mertz et al. (1996) investigated evaporation of water and R-141b in small vertical channels (single- and multi-channel elements) that were from 1 to 3 mm wide with aspect ratios up to 3. Their multi-channel test sections had various numbers of channels: 101 channels (1 mm wide), 50 channels (2 mm wide) and 33 channels (3 mm wide), all fitted with a glass cover plate. Their single-channel and the multi-channel tests showed similar flow patterns: single bubble flow, confined bubble flow and annular flow. Fluctuations of the two-phase flow in the multi-channel elements were also evident, as well as maldistribution of the phases (some channels filled with vapor at high heat flux conditions while others did not).

Yang and Shieh (2001) compared their flow pattern observations for adiabatic air–water flows versus flow boiling of R-134a in small circular horizontal tubes ($D = 1$ (water only), 2 and 3 mm) and reported seeing six individual flow regimes: bubbly flow, plug flow, wavy flow, slug flow, annular flow and dispersed flow. They proposed a flow pattern map based on liquid velocity versus gas velocity, in which the flow pattern transitions for R-134a could be observed quite clearly but not those for air–water.

Coleman and Garimella (1999, 2000) also proposed flow pattern maps for their numerous air–water and R-134a observations in various round and square channels, presenting their observations in a G versus x format. They showed numerous images to define their flow regime classifications, which is very helpful to the reader. Their channel dimensions ranged from 1 to 4 mm and hence they observed some stratified flows for some test conditions.

While still other flow pattern observations are reported in the literature and also various tentative flow pattern maps, there is still a lot of additional research required before a reasonably reliable prediction of flow pattern transition boundaries in microchannel flows can be made, both for circular and non-circular channels. For microchannel two-phase flows without stratification, a case can probably be made that only bubbly, elongated bubble, annular and mist flows and flows with partial dryout are sufficient to capture most of the physics involved, with practical thermal design methods in mind. For evaporating flows, the bubbly flow regime lifespan (that is, bubbles notably smaller than the channel size) is very short as bubbles grow to the channel size very quickly, typically within a few centimeters of tube length or less.

5. Flow boiling heat transfer studies

The review here will be limited to a representative description of some of the single-channel flow boiling heat transfer studies reported in the literature, i.e. those sufficient to illustrate the typical trends observed in these types of data. Also, the preference here is to discuss circular tube tests as opposed to those for narrow rectangular channels with only part of the perimeter heated. A growing number of multi-channel studies have also been performed but there is not space here to cover these.

In a systematic study at Argonne Laboratory, Wambsganss et al. (1993) reported results for R-113 evaporating in a circular channel of 2.92 mm diameter while Tran et al. (1996) reported corresponding results for R-12 evaporating in a 2.46 mm circular channel. At wall superheats larger than 2.75 K, they noted that the local heat transfer coefficients did not change with mass velocity (over the range from 50 to 695 kg/m^2 s) nor with vapor quality (from 20% to 75%) but were dependent on heat flux (from 7.5 to 59.4 kW/m^2). Consequently, applying macroscale logic, they concluded that heat transfer was always nucleate boiling dominated in microchannel evaporation and fitted their data to a nucleate boiling curve (of the form $q = a\Delta T^n$, where ΔT is the wall superheat and q is the heat flux), obtaining an exponent of $n = 2.7$ typical of nucleate pool boiling correlations. At lower superheats (below 2.75 K), they observed a significant change in the slope of their data plotted as a nucleate boiling curve (q versus ΔT), and this they designated as a convection-dominant regime (even though it was only heat flux dominated). Fig. 2 shows some of their results with heat transfer coefficient plotted versus vapor quality.

Zhao et al. (2000) reported flow-boiling coefficients for CO_2 and R-134a in a microchannel of unspecified

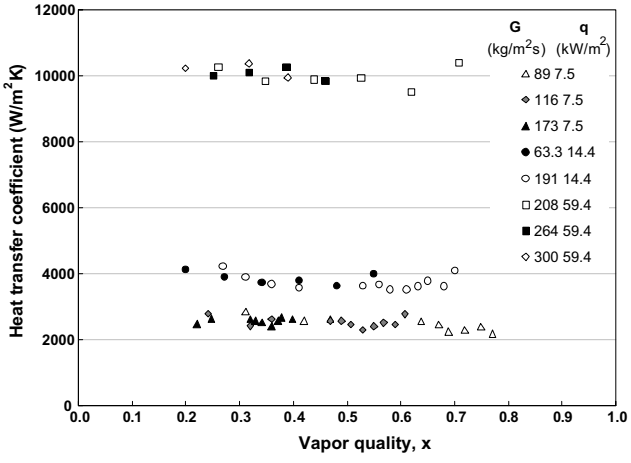

Fig. 2. Flow boiling data for R-12 in 2.46 mm tube of Tran et al. (1996).

dimensions for vapor qualities from 5% to 30%. For mass velocities from 250 to 700 kg/m^2 s at fixed heat fluxes, no mass-flux dependence was observed on the flow boiling heat transfer coefficients for either CO_2 or R-134a for pressures ranging from 4.0 to 5.1 bar and 0.35 to 0.49 bar, respectively. In their heat flux range (8 to 25 kW/m^2), their results did not show any *heat flux* dependence, in contrast to the study above. This may have been because these tests were for small wall superheats (1–2 K). Hence, their data would have fallen in the lower heat-flux dependence zone observed by Tran and co-workers. For the same saturation temperature (283 K), CO_2 had heat transfer coefficients about two to three times those of R-134a.

Bao et al. (2000) reported local flow boiling coefficients for R-11 and R-123 inside a copper tube with a diameter of 1.95 mm. They used a single piece of tubing, 870 mm long. The first 400 mm of the tube was unheated, providing an entrance region; that section was followed by a 270 mm long test zone and then by a 200 mm unheated exit zone. For tests over a wide range of conditions (mass velocities from 50 to 1800 kg/m^2 s, vapor qualities from 0% to 90%, heat fluxes from 5 to 200 kW/m^2 and saturation pressures from 290 to 510 kPa), they observed that heat transfer coefficients were a strong function of heat flux and increased with saturation pressure; however, the effects of vapor quality and mass flux were very small. Hence, similar to the previous studies, they concluded that nucleate boiling dominated the heat transfer process. In fact, they demonstrated that the Cooper (1984) correlation gave an approximate representation of their data (although it underpredicted their results by 20–50%). Using the same type of setup, Baird et al. (2000) also reported local heat transfer data for R-123 in a 0.92-mm-diameter tube and CO_2 in the previous 1.95 mm tube, observing the same trends as before.

Fig. 3 shows some of their local heat transfer coefficients (h_{exp}) plotted versus vapor quality including the subcooled boiling data. Fig. 4 shows their saturated boiling data plotted versus heat flux. Fig. 5 depicts some of their results plotted for various saturation pressures. These results essentially reinforce the above conclusion that microchannel flow boiling heat transfer coefficients at these test conditions are not a function of *vapor quality* nor *mass velocity* (in complete contrast to macrochannel trends) but are a function of *heat flux* and *saturation pressure*, just like occurs in nucleate pool boiling.

Hwang et al. (2000) measured flow boiling heat transfer coefficients for R-134a in a 2.2 mm stainless steel tube at heat fluxes ranging from 19 to 64 kW/m^2 and mass velocities of 280, 470 and 570 kg/m^2 s. Based on the flow pattern maps of Damianidis and Westwater (1987) and Wambsganns et al. (1997), they classified most of their experimental data in the slug and annular

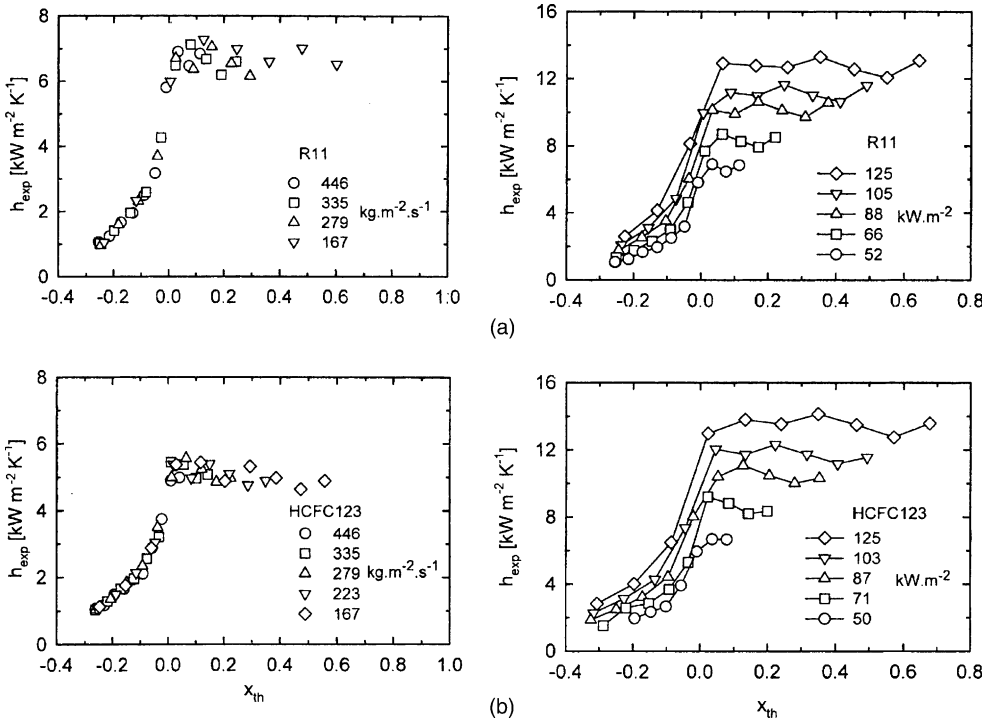

Fig. 3. Flow boiling data for R-11 and R-123 in 1.95 mm tube of Bao et al. (2000) plotted versus vapor quality, (a) influence of mass flux, (b) influence of heat flux.

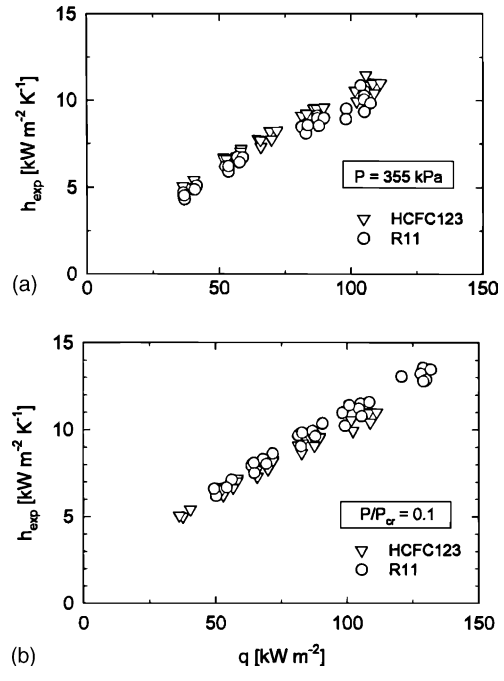

Fig. 4. Flow boiling data for R-11 and R-123 in 1.95 mm tube of Bao et al. (2000) plotted versus heat flux.

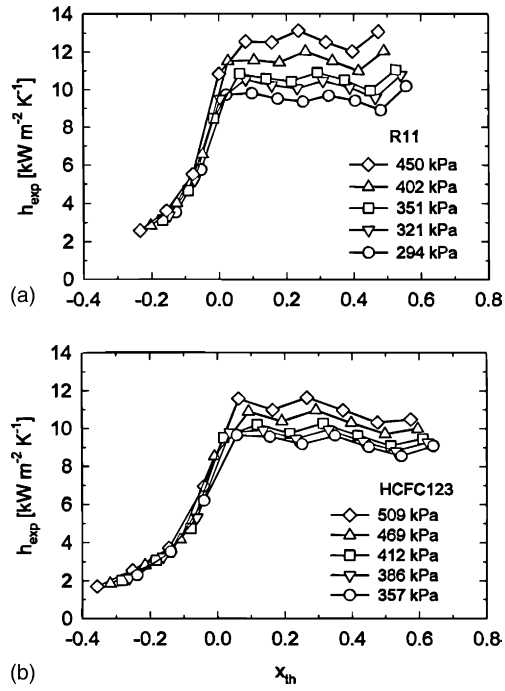

Fig. 5. Flow boiling data for R-11 and R-123 in 1.95 mm tube of Bao et al. (2000) at various saturation pressures.

flow regimes. The results depicted an influence of heat flux (as expected from the above comments) but also an effect of mass velocity (not expected from the above), for a wide range of vapor qualities.

Lin et al. (2001) studied evaporation of R-141b in a vertical 1.1 mm (paper also says 1 mm) tube over a mass velocity range of 300–2000 kg/m^2 s and heat flux range of 18–72 kW/m^2, although they only presented data at

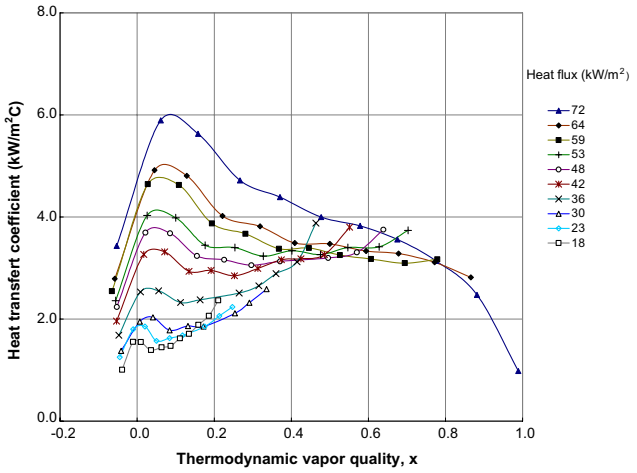

Fig. 6. Flow boiling data for R-141b in 1.1 mm tube of Lin et al. (2001).

the mass velocity of 510 kg/m^2 s. Fig. 6 depicts their results for heat transfer versus vapor quality at these conditions. The outlet pressure of the test section was atmospheric while the inlet pressure varied from 1.35 to 2.20 bar depending on the flow conditions, which means the data shown also include a small saturation pressure effect. As opposed to most of the above studies, they found a significant influence of vapor quality on the heat transfer coefficient. At high heat fluxes, their data illustrated a sharp peak at low vapor qualities followed by a monotonic decrease; at low heat fluxes, there was a significant monotonic rise in value up to a peak at about $x = 0.60$; at intermediate heat fluxes, such 42 and 48 kW/m^2, the heat transfer coefficients were nearly independent of vapor quality as in previous investigations. Hence, these results present a much more complex dependency of the heat transfer coefficient on heat flux and vapor quality than those noted above. In the subcooled region, i.e. $x < 0.0$, the heat transfer coefficients are much larger than those calculated from a single-phase correlation and are similar to the Bao et al. (2000) data shown earlier. Consequently, subcooled evaporation is taking place before the saturated zone in these tests, which may have an influence on the two-phase flow downstream.

Summarizing the results above, most support the thesis that microchannel flow boiling heat transfer coefficients are *not* a function of vapor quality *nor* mass flux (in complete contrast to macrochannel trends) but *are* a function of heat flux and saturation pressure. These experimentalists concluded, applying macroscale logic, that flow heat transfer in microchannels is controlled by nucleate boiling. On the other hand, the studies of Lin et al. (2001) and Hwang et al. (2000) demonstrate significant effects of vapor quality and mass velocity, respectively. Hence, the complete picture of the "heat transfer map" for evaporation in microfin tubes has yet to be established. Furthermore, in the next section, the heat transfer model proposed by Jacobi and Thome (2002) demonstrates that nucleate boiling is not the dominant heat transfer mechanism.

Various experimental considerations need to be addressed concerning the integrity of microchannel evaporation data. Many of the published studies have not proven that they could satisfactorily measure single-phase laminar or turbulent flow heat transfer coefficients prior to their flow boiling tests. This is an important benchmark test that should not be neglected. Secondly, if nucleate boiling is so important as many of these studies suggest, then the internal surface roughness of the microchannel has an important influence on the heat transfer data and should be measured and reported. Thirdly, no concerted comparison between independent data for the same fluid, same tube diameter, same test conditions, etc. has been made to double-check the *universality* of the data (also, it is important to show that the data are reproducible from day-to-day in the same test section, which was always a problem with many nucleate pool boiling studies). Fourthly, if the pressure drops are very large in the test sections, then the flashing effect on the enthalpy change has to be taken into account when determining and reporting the local vapor quality. Fifthly, there is still an open question regarding the influence of the inlet conditions of the test section on the measured data; some have subcooled boiling prior to the test section while some do not, which may or may not significantly influence the structure of the two-phase flow going through the test section. Sixthly, only a few of the papers address the issue of steady-state or instability of the flow, which seems to be an experimental challenge to achieve. For instance, Lin et al. (2001) presented a graph to document the notable temperature fluctuations measured during their tests at three heat flux levels. Many of the studies cited here have attempted to address some of these six points. In the future, we need to pay closer attention to all the experimental details and measurement strategy issues to make sure we are obtaining the data correctly and not unknowingly adversely influencing the results.

Other issues important to evaporation in microchannels are onset of boiling (nucleation), critical heat flux, non-circular channels, non-uniform heating, multichannel effects and so forth. These are not addressed here (refer to the other reviews cited earlier).

6. Evaporation models

First of all, let us address the issue of application of macroscale models to microchannel evaporation. Macroscopic flow boiling heat transfer models are of three types, the Chen summation models, the asymptotic models and the flow pattern based models. For the first

type, Chen (1966) proposed the following expression for the local flow boiling heat transfer coefficient

$$h_{tp} = h_{nb}S + h_L F \tag{6}$$

where the contributions of nucleate boiling and convective evaporation are additive, but corrected by a nucleate boiling suppression factor S and a two-phase convection multiplier F. The nucleate boiling coefficient h_{nb} was obtained with the Forster–Zuber pool boiling correlation and the convective boiling contribution was obtained using the classic Dittus–Boelter heat transfer correlation for single-phase turbulent convection in a tube to get h_L. Numerous others have since proposed variations of this model. However, if the term $h_L F$ is small with respect to $Sh_{nb,FZ}$, then these types of correlations give the appearance of representing microchannel test data that are only a function of heat flux and saturation pressure. However, they are not able to explain microchannel data that display an effect of vapor quality or mass velocity, such as those of Lin et al. (2001). Furthermore, these methods used a *turbulent* flow correlation for h_L while most microchannel flow boiling data have liquid Reynolds numbers below 2300 and hence these methods are not applicable to *laminar* flow boiling. In addition, the suppression factor S was developed for a turbulent boundary layer and thus cannot be applied blindly to boiling nucleation in laminar flows. Thus, it is illogical to apply or empirically adapt such methods to microchannel evaporation since they probably will only fit that data set but not be very reliable for general application.

Regarding asymptotic models, for instance the Steiner and Taborek (1992) expression for vertical tubes is

$$h_{tp} = (h_{nb}^3 + h_L^3)^{1/3} \tag{7}$$

where in this case the Gnielinski transition-turbulent flow correlation for single-phase flows in tubes is used to obtain h_L. As above, it does not make sense to apply such a method to microchannel evaporation involving laminar flows, although its underlying database is for tube diameters from 1 to 32 mm.

With respect to the flow pattern based flow boiling model of Kattan et al. (1998a,b,c) for horizontal tubes, it predicts the local flow boiling heat transfer coefficient as a function of the fraction of the tube perimeter wetted by the fluid and the flow regime. Flow boiling occurs on the wetted perimeter and vapor-phase forced convection occurs on the dry perimeter (if any). The local flow boiling coefficient h_{tp} for evaporation in a macroscale horizontal, plain tube is given by:

$$h_{tp} = \frac{r_i \theta_{dry} h_{vapor} + r_i(2\pi - \theta_{dry})h_{wet}}{2\pi r_i} \tag{8a}$$

where the internal tube radius is r_i, the dry perimeter of the tube, if any, is given by $r_i\theta_{dry}$ and θ_{dry} is the dry angle around the top of the tube. On the wetted perimeter of the tube, $[r_i(2\pi - \theta_{dry})]$, the heat transfer coefficient is h_{wet}, which is obtained from an asymptotic expression that combines the nucleate boiling h_{nb} and convective boiling h_L contributions to heat transfer as above:

$$h_{wet} = (h_{nb}^3 + h_L^3)^{1/3} \tag{8b}$$

In this model, the convective boiling heat transfer coefficient h_L is obtained with a *film* flow model and the local void fraction. For annular and intermittent flows, $h_{tp} = h_{wet}$. Once again, this method could be applied to microchannels when h_{nb} dominates but their flow pattern map is not applicable to microscale flows and their film flow correlation for h_{cb} is for turbulent films, not laminar films.

Thus, in summary, while some macroscale flow boiling methods may sometimes give a reasonable statistical fit to microchannel flow boiling data, this is probably only by chance. It would be better to have a new method that incorporates features of the physical process of microchannel flow and evaporation, which would then perhaps lead to the development of a general design method.

Along this line of thinking, as opposed to the previously mentioned experimental studies that concluded that microchannel evaporation is controlled by nucleate boiling, Jacobi and Thome (2002) have shown that the transient thin film evaporation heat transfer mechanism in the elongated bubble mode can explain the same trends and, because it gives a physical description of the flow, concluded that this mechanism is controlling, not nucleate boiling. To prove this, they proposed an analytical model to describe evaporation in microchannels in the elongated bubble flow regime. They concentrated on the transient thin film evaporation mechanism in the liquid films trapped between the wall and passing bubbles. Fig. 7 depicts the flow geometry assumed in their model where δ_o is the initial liquid film thickness laid down by the liquid slug, D is the internal diameter of the tube, L_V is the length of the growing elongated bubble, L_L is the length of the liquid slug between bubbles and L_p is the total length of one slug/bubble pair. The frequency of the bubbles was obtained from the successive nucleation and growth of bubbles across the flow channel and their subsequent departure, bubbles which then flowed downstream and elongated during their growth, with the vapor provided by thin film evaporation of the liquid film trapped between the bubble and the heated channel. Hence, as the liquid in the slug is entrained into the film and the film evaporates, the length L_L decreases and the length L_V increases. The local liquid film thickness δ decreases with time as transient thin film evaporation progresses, up until the next liquid slug arrives. In this two-zone model, the heat transfer to the laminar flow of the liquid slug zone was found to be negligible compared with the elongated bubble zone and was thus ignored, effectively reducing

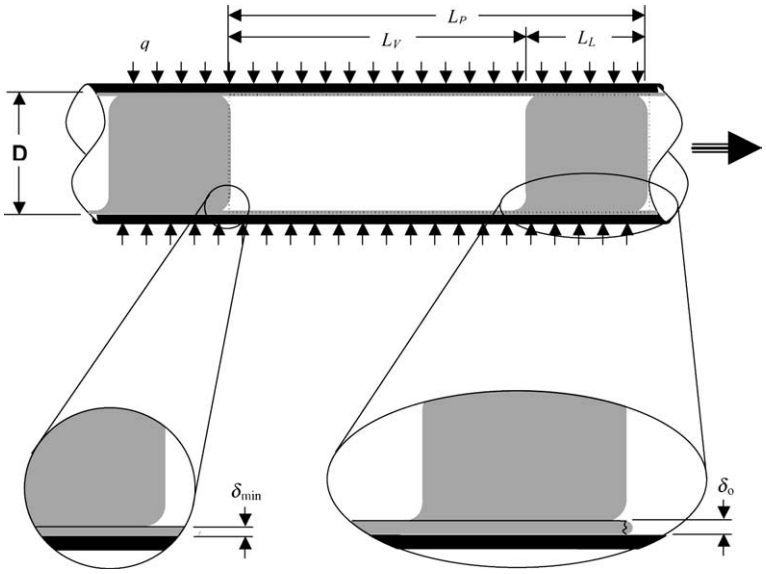

Fig. 7. Microchannel evaporation geometry of Jacobi and Thome (2002) for an elongated bubble and liquid slug pair.

this to a one-zone model. To implement their model for a particular microchannel diameter, a nucleation radius must be assumed to obtain the nucleation superheat ΔT_{nuc} and an initial value for δ_o must be chosen as no method was available to predict its value. Parametric studies showed that the model predicted several independent experimental sets described earlier quite well when they assumed that the film thicknesses were on the order of 10–20 μm for channels 2.5 mm in size or smaller.

One might try to argue that thin film evaporation around an elongated bubble is nucleate boiling, i.e. microlayer evaporation underneath a growing bubble, but the similarity ends there as most of the heat leaves a nucleate pool boiling surface in the form of sensible heat, cf. Nakayama et al. (1980) who measured these contributions, via the thermal boundary layer stripping mechanism and bubble agitation mechanism while the convection contribution of the liquid slug is negligible in a microchannel.

At the test conditions of Bao et al. (2000), Fig. 8 shows that based on these assumptions, the Jacobi–Thome model predicts the local heat transfer coefficient to be only a weak function of mass velocity, depending on the nucleation superheat (or nucleation radius) and the initial film thickness chosen. Similarly, at a fixed mass velocity and heat flux, Fig. 9 shows that the model predicts the local heat transfer coefficient not to be a function of vapor quality but to increase with saturation pressure, similar to the original data in Fig. 5 for $x > 0$. Also, the model predicts the Bao et al. (2000) data quite well as shown in Fig. 10, if the optimal nucleation superheat (or nucleation radius) and film thickness are assumed, but something is still amiss since the trend of the data do not match that of the prediction curve. The

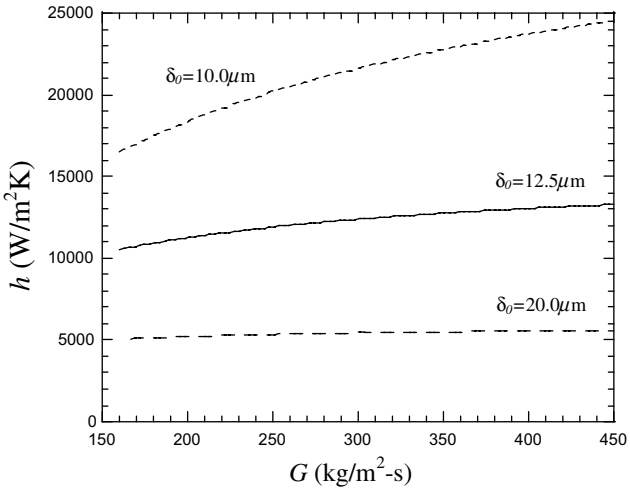

Fig. 8. Heat transfer versus mass velocity predicted for R-11 at $P_{sat} = 460$ kPa, $D = 2$ mm and $q = 120$ kW/m^2 for varying δ_o at a fixed $\Delta T_{nuc} = 28$ K ($r_{nuc} = 0.07$ μm).

model also predicted data of several other authors for other fluids with some success. While this model is only partially complete (i.e. values of two parameters must be assumed), its objective was to prove that microchannel evaporation heat transfer is largely influenced by the transient thin film evaporation heat transfer mechanism, not nucleate boiling.

Currently, Thome et al. (2004) are developing a new three-zone elongated bubble flow model that includes a method for predicting the initial film thickness δ_o as a function of the flow variables, the onset of dryout and dryout heat transfer, plus several other new features of the flow. So far, this new model can explain *qualitatively* all the experimental trends noted above, even those in the data of Lin et al. (2001), and for now is in reasonable

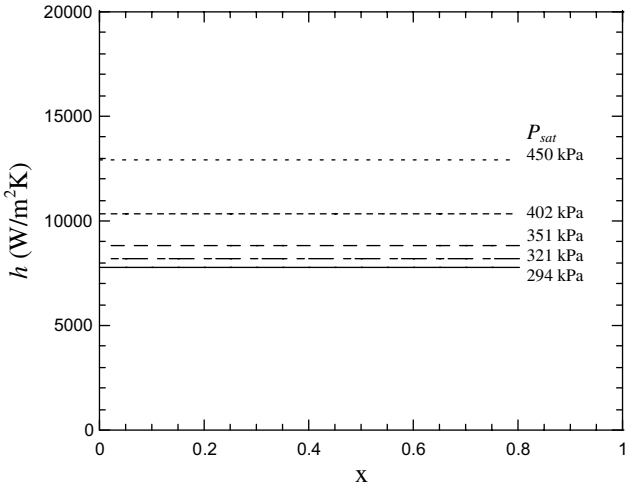

Fig. 9. Predicted heat transfer coefficients for R-11 as a function of vapor quality with $\Delta T_{nuc} = 28$ K and $\delta_o = 12.5$ μm at various P_{sat} (r_{nuc} from 0.12 to 0.06 μm), $q = 125$ kW/m^2 and $G = 560$ kg/m^2 s to cover the conditions reported by Bao et al. (2000).

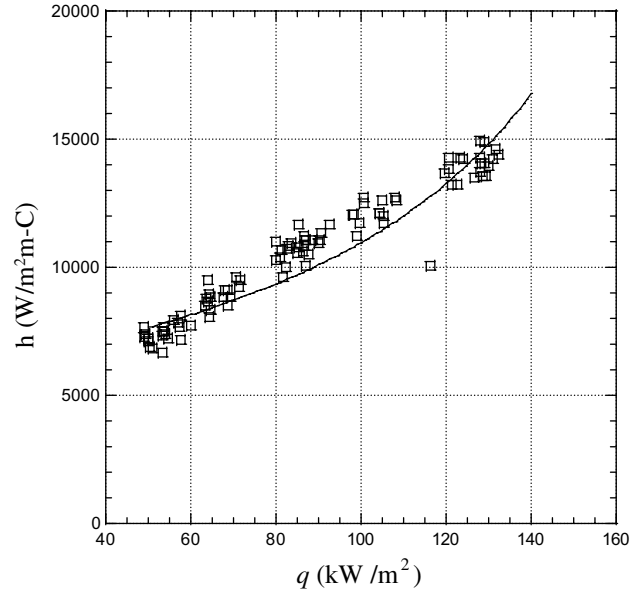

Fig. 10. Comparison of the Jacobi–Thome model to the data of Bao et al. (2000) for R-11 at $P_{sat} = 460$ kPa at all mass velocities with the model parameters set to $\Delta T_{nuc} = 28$ K ($r_{nuc} = 0.070$ μm) and $\delta_o = 12.5$ μm.

quantitative agreement (67% of the data predicted within ±30%) with a large independent database for seven different fluids, considering also the difficulties in making these measurements noted earlier. Even so, numerous new challenges to describing the boiling process come to light as the research community delves deeper into the physics of microchannel two-phase flow and evaporation. Thus, there is still the need for extensive future research to resolve the fundamentals such that more accurate phenomenological models can be developed in the future for all the pertinent flow regimes.

7. Conclusions

Experiments and theory on evaporation in microchannels have been reviewed. What best defines a microchannel is not yet clear but the threshold to confined bubble flow is a good working definition for the upper limit while the lower limit may be the complete suppression of nucleation and hence the threshold to nanochannels, from a two-phase flow and heat transfer perspective anyway. The primary flow regimes observed are elongated bubble flow (also referred to as slug flow or confined bubble flow) and annular flow while some observers also report observing bubbly flow and several other regimes, such as liquid ring flow and liquid lump flow, which are probably transition regimes. Flow boiling heat transfer coefficients have been shown experimentally to be dependent nearly exclusively on heat flux and saturation pressure, i.e. similar to nucleate pool boiling heat transfer and only slightly dependent on mass velocity and vapor quality. This has led to the conclusion that nucleate boiling controls evaporation in microchannels. Instead, in a new elongated bubble flow heat transfer model, Jacobi and Thome (2002) have shown that transient evaporation of the thin liquid films surrounding elongated bubbles is the dominant heat transfer mechanism. More recent tests also demonstrate a mass velocity and vapor quality effect. In conclusion, the state-of-the-art of two-phase flow and heat transfer in microchannels is still in its infancy and much fundamental experimental and analytical work remains to be done.

Acknowledgements

This work was supported in part by the Swiss National Science Foundation grant 2000021-101597/1.

References

Baird, J.R., Bao, Z.Y., Fletcher, D.F., Haynes, B.S., 2000. Local flow boiling heat transfer coefficients in narrow conduits. In: Bar-Cohen, A. (Ed.), Boiling 2000: Phenomena and Engineering Applications, Anchorage Alaska, 30 April–5 May, vol. 2, pp. 447–466.

Baker, O., 1954. Simultaneous Flow of Oil and Gas. J. Oil and Gas 53, 85–195.

Bao, Z.Y., Fletcher, D.F., Haynes, B.S., 2000. Flow boiling heat transfer of freon R11 and HFCFC123 in narrow passages. Int. J. Heat Mass Transfer 43, 3347–3358.

Bergles, A.E., Lienhard V, J.H, Kendall, G.E., Griffith, P., 2003. Boiling and evaporation in small diameter channels. Heat Transfer Engineering 24 (1), 18–40.

Chen, J.C., 1966. A correlation for boiling heat transfer to saturated fluids in convective flow. I&EC Process Des. Develop. 5 (3), 322–329.

Coleman, J.W., Garimella, S., 1999. Characterization of two-phase flow patterns in small diameter round and rectangular tubes. Int. J. Heat Mass Transfer 42, 2869–2881.

Coleman, J.W., Garimella, S., 2000. Two-phase flow regime transitions in microchannel tubes: the effect of hydraulic diameter. In: Proceedings of ASME Heat Transfer Division-2000, ASME IMECE 2000, vol. 4, pp. 71–83.

Cooper, M.G., 1984. Heat flow rates in saturated nucleate boiling—A wide ranging examination using reduced properties. In: Advances in Heat Transfer, Academic Press, Princeton, Vol. 16, pp. 157–239.

Collier, J.G., Thome, J.R., 1994. Convective Boiling and Condensation, 3rd ed. Oxford University Press, Oxford, England.

Cornwell, K., Kew, P.A., 1993. Boiling in small parallel channels. In: Pilavachi, P.A. (Ed.), Energy Efficiency in Process Technology. Elsevier, pp. 624–640.

Cornwell, K., Kew, P.A., 1995. Evaporation in microchannel heat exchangers. In: Proceedings of Fourth UK National Conference on Heat Transfer, pp. 289–293.

Damianidis, C.A., Westwater, J.W., 1987. Two-phase flow patterns in a compact heat exchanger and in small tubes. In: Proceedings of Second UK National Conference on Heat Transfer, vol. 2, pp. 1257–1268.

Feng, Z., Serizawa, A., 2000. Two-phase flow patterns in ultra-small-channels. In: Second Japanese–European Two-Phase Flow Group Meeting, Tsukuba, Japan.

Fritz, W., 1935. Berechnung des maximal Volume von Dampfblasen. Phys. Z. 36, 379–388.

Huo, Y., Tian, Y.S., Wadekar, V.V., Karayiannis, T.G., 2001. Review of aspects of two-phase flow and boiling heat transfer in small diameter tubes. In: Proceedings of Third International Conference on Compact Heat Exchangers and Enhancement Technology for the Process Industries, Davos, Switzerland, pp. 335–346.

Hwang, Y.-W., Kim, M.S., Ro, S.T., 2000. Experimental investigation of evaporative heat transfer characteristics in a small-diameter tube using R134a. In: Proceedings of Symposium on Energy Engineering in the 21st Century, Hong Kong, vol. 3, pp. 965–971.

Jacobi, A.M., Thome, J.R., 2002. Heat transfer model for evaporation of elongated bubble flows in microchannels. J. Heat Transfer 124, 1131–1136.

Kandlikar, S.G., 2001. Two-phase flow patterns, pressure drop and heat transfer during boiling in minichannel and microchannel flow passages of compact heat exchangers. In: Compact Heat Exchangers and Enhancement Technology for the Process Industries—2001, Begell House, New York, pp. 319–334.

Kandlikar, S.G., Grande, W.J., 2003. Evolution of microchannel flow passages—thermohydraulic performance and fabrication technology. Heat Transfer Eng. 24 (1), 3–17.

Kasza, K.E., Didascalou, T., Wambsganss, M.W., 1997. Microscale flow visualization of nucleate boiling in small channels: mechanisms influencing heat transfer. In: Shah, R.K. (Ed.), Proceedings of International Conference on Compact Heat Exchangers for Process Industries, Begell House, New York, pp. 343–352.

Kattan, N., Thome, J.R., Favrat, D., 1998a. Flow boiling in horizontal tubes. Part 1: Development of a diabatic two-phase flow pattern map. J. Heat Transfer 120, 140–147.

Kattan, N., Thome, J.R., Favrat, D., 1998b. Flow boiling in horizontal tubes. Part 2: New heat transfer data for five refrigerants. J. Heat Transfer 120, 148–155.

Kattan, N., Thome, J.R., Favrat, D., 1998c. Flow boiling in horizontal tubes. Part 3: Development of a new heat transfer model based on flow patterns. J. Heat Transfer 120, 156–165.

Kew, P., Cornwell, K., 1997. Correlations for prediction of boiling heat transfer in small diameter channels. Appl. Thermal Eng. 17 (8–10), 705–715.

Kuwahara, K., Koyama, S., Yu, J., Watanabe, C., Osa, N., 2000. Flow pattern of pure refrigerant HFC134a evaporating in a horizontal capillary tube. In: Proceedings of Symposium on Energy Engineering in the 21st Century, Hong Kong, vol. 2, pp. 445–450.

Lin, L., Pisano, A.P., 1991. Bubble forming on a micro line heater, micromechanical sensors, actuators and systems. ASME DSC 32, 147–164.

Lin, S., Kew, P.A., Cornwell, K., 2001. Two-phase heat transfer to a refrigerant in a 1 mm diameter tube. Int. J. Refrig. 24, 51–56.

Mehendal, S.S., Jacobi, A.M., Shah, R.K., 2000. Fluid flow and heat transfer at micro- and meso-scales with application to heat exchanger design. Appl. Mech. Rev. 53 (7), 175–193.

Mertz, R., Wein, A., Groll, M., 1996. Experimental investigation of flow boiling heat transfer in narrow channels. In: Second European Thermal Sciences and 14th UIT National Heat Transfer Conference, Rome, May 26–31.

Nakayama, W., Kaikoku, T., Kuwahara, H., Nakajima, T., 1980. Dynamic model of enhanced boiling heat transfer on porous surfaces, Part I: experimental investigation. J. Heat Transfer 102, 445–450.

Sheng, C.-H., Palm, B., 2000. The visualisation of boiling in small diameter tubes. In: Proceedings of Heat Transfer and Transport Phenomena in Microscale, pp. 204–208.

Steiner, D., Taborek, J., 1992. Flow boiling heat transfer in vertical tubes correlated by an asymptotic model. Heat Transfer Eng. 13 (2), 43–69.

Taitel, Y., Dukler, A.E., 1976. A model for predicting flow regime transitions in horizontal and near horizontal gas–liquid flow. AIChE J. 22, 47–55.

Thome, J.R., Groll, M., Mertz, R., 2003. Microscale heat transfer: boiling and evaporation (Section 2.13.4), in Heat transfer and fluid flow in microchannels (Chapter 2.13). In: Heat Exchanger Design Update. Begell House, New York, pp. 2.13.4.1–27.

Thome, J.R., Dupont, V., Jacobi, A.M., 2004. Heat transfer model for evaporation in microchannels, Part I: Presentation of the model. Int. J. Heat Mass Transfer, 47, in press.

Tran, T.N., Wambsganss, M.W., France, D.M., 1996. Small circular and rectangular channel boiling with two refrigerants. Int. J. Multiphase Flow 22 (3), 485–498.

Triplett, K.A., Ghiaasiaan, S.M., Abdel-Khalik, S.I., Sadowski, D.L., 1999. Gas–liquid two-phase flow in micro-channels, Part I: Two-phase flow patterns. Int. J. Multiphase Flow 25, 337–394.

Wambsganss, M.W., France, D.M., Jendraejczyk, J.A., Tran, T.N., 1993. Boiling heat transfer in a horizontal small-diameter tube. J. Heat Transfer 115, 963–972.

Wambsganns, M.W., Shah, R.K., Celata, G.P., Zummo, G., 1997. Vaporization in compact heat exchangers. In: Proceedings of Fourth World Conference on Experimental Heat Transfer, Fluid Mechanics and Thermodynamics, vol. 4, pp. 2049–2062.

Yang, C.-Y., Shieh, C.-C., 2001. Flow pattern of air–water and two-phase R134a in small circular tubes. Int. J. Multiphase Flow 27, 1163–1177.

Zhao, Y., Molki, M., Ohadi, M.M., Dessiatoun, S.V., 2000. Flow boiling of CO_2 in microchannels. ASHRAE Trans. 106 (1), 437–445.